ELSEVIER

Nuclear Instruments and Methods in Physics Research A 414 (1998) 317–324

NUCLEAR INSTRUMENTS & METHODS IN PHYSICS RESEARCH Section A

Streamer suppression with SF_6 in RPCs operated in avalanche mode

P. Camarri[a], R. Cardarelli[a], A. Di Ciaccio[a], R. Santonico[a]

[a] *Dipartimento di Fisica, Università di Roma "Tor Vergata" and INFN, Sezione di Roma II, Via della Ricerca Scientifica, 1, I-00133 Rome, Italy*

Received 9 February 1998

Abstract

We show that the addition of small amounts of sulphur hexafluoride, SF_6, to the present ATLAS baseline gas mixture $C_2H_2F_4/C_4H_{10}$ has a very strong effect in suppressing the avalanche-to-streamer transition. An RPC of $50 \times 50\,cm^2$ area, 2 mm gas gap was operated in pure avalanche, streamer-free mode in a voltage range of about 1 kV. The results of the test suggest that the observed fast signal could be interpreted as the sum of contributions of a number of primary saturated avalanches.

Keywords: Resistive plate chambers; Gaseous detectors; Streamer suppression; Sulphur hexafluoride (SF_6)

1. Introduction

The avalanche and streamer operating modes in Resistive Plate Chambers, RPCs, can be characterized in the plot showing the charge pulse, in logarithmic scale, vs. the operating voltage [1]. For an avalanche discharge this plot is characterized by a linear region typical of the Townsend exponential discharge where the gas gain is very strongly dependent on the operating voltage, followed by a relatively flat region with a much weaker gas gain dependence on the operating voltage, indicating a saturation of the avalanche possibly due to space charge effects.

For most gases, including the one of Ref. [1], the voltage range in which an RPC can be operated in avalanche mode is limited by the appearance of the streamer. This is normally a non-wanted phenomenon which, in addition of increasing drastically the delivered charge, also produces high pick-up strip multiplicities as expected from the very low discrimination threshold that is required by the avalanche operation.

In the present paper we show that the addition of SF_6 amounts in the 1% range to the mixture $C_2H_2F_4/C_4H_{10} = 97/3$, has the effect of suppressing the streamer in a very large interval of operating voltages. The absence of streamers makes the avalanche working mode, in the saturation region, extremely attractive for RPCs with digital readout.

2. Experimental set-up

This paper describes a cosmic ray test made in the INFN laboratories of Roma 2 by means of an

0168-9002/98/$19.00
PII: S0168-9002(98)00576-2

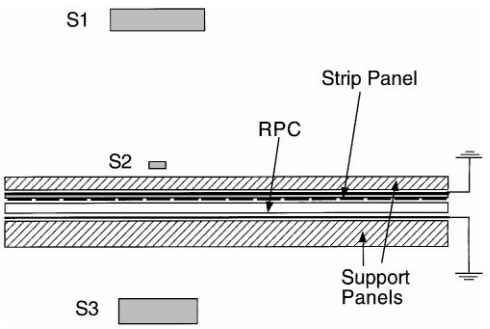

Fig. 1. Experimental layout: scintillator telescope and details of the test RPC; digital oscilloscope and DAQ system.

experimental set-up similar to the one already described in Ref. [1]. A set of three scintillators S1, S2 and S3 are used to select a cosmic ray beam intersecting the RPC under test. Two scintillators, S1 and S3, have relatively large sizes, $60 \times 10\,cm^2$ and $50 \times 8.5\,cm^2$, with respect to the RPC pick up strips, while the third one is a "finger" of $2 \times 30\,cm^2$, 1 cm thick. The RPC of $50 \times 50\,cm^2$ sensitive area, has a 2 mm gap between 2 mm bakelite plates, according to the scheme of the ATLAS Muon TDR [2].

The read out is made of 16 aluminum strips glued on a plate of expanded polystyrene 3 mm thick which has a grounded aluminum foil glued on the opposite face. Thin grounded copper wires are inserted between contiguous strips. The strips, which have an impedance of 25 Ω, are terminated at both ends. At the end where the signal is read out the termination is realized by a 50 Ω resistor in parallel with a 50 Ω cable feeding 1/2 of the signal current into the amplifier. The experimental set-up and the RPC lay out are sketched in Fig. 1.

The data taking of the test was made using a 4 channel digital oscilloscope of 1 GHz analog bandwidth which sampled 500 points per signal at a sampling speed up to 5 Gsample/s. The oscilloscope was triggered on throughgoing cosmic rays using the triple coincidence signal of the scintillator telescope and for each trigger the signal waveforms of three consecutive pick up strips were recorded. The scintillator finger was centered over the middle strip. Due to the geometrical acceptance of the telescope, the cosmic ray trajectory intersected sometimes the region between two contiguous strips and the signal was shared between them.

The data acquisition was managed by a personal computer which recorded the waveforms of the three strips.

The gas was the mixture $C_2H_2F_4/C_4H_{10} = 97/3$, with the addition of a small amount of SF_6. We tried 5%, 2% and 1% of SF_6; the binary mixture without SF_6 was also tested for reference.

For each gas we scanned a voltage range of at least 2 kV. At operating voltages below the streamer threshold the oscilloscope horizontal scale was set at 10 ns/cm and a typical avalanche signal was measured by about 40 sample points. Above the streamer threshold the time scale was set at 50 ns/cm so that delayed streamers up to about 500 ns were detectable. The corresponding sampling frequency was only 1 Gsample/s and a typical avalanche signal was measured with only about 8 sample points, a rather modest number that made the avalanche measurements obtained in these conditions significantly poorer. The fraction of streamers expected after 500 ns was completely negligible for all the tested gases.

The signals of the three strips were amplified using a voltage amplifier of gain 25, frequency bandwidth 500 MHz, input impedance 50 Ω and equivalent noise of 6 dB. At very low voltage, where the signal amplitude was only a fraction of a millivolt, two cascaded amplifier stages were used, whereas above the streamer threshold no amplifier was used to avoid saturation effects due to large signals.

In our search for streamer suppressing gases we also tested, for completeness, the binary mixture C_2HF_5/C_4H_{10}[3] with 2% and 6% of butane. The experimental results are given in the next paragraph for all tested gases.

We also made a parallel and independent measurement of the RPC detection efficiency using the RPC front-end electronics that has been developed for ATLAS. This frontend circuit [4] consists of a voltage amplifier coupled to a discriminator. The amplifier has a frequency bandwidth of 160 MHz with a gain of 300 at 100 MHz and an input impedance of 50 Ω. The amplified signal is fed into a standard discriminator with threshold adjustable from 30 mV to 1 V. This frontend circuit,

already used in many beam tests of RPCs [5–7], is made with standard commercial components. The same circuit has been also integrated in a GaAs chip [8] but the latter one was not used in the present test.

The front-end board was fixed at one end of the strip plane, on the opposite side of the end connected to the oscilloscope. Also in this case the 25 Ω impedance of the pick up strip was matched using a 50 Ω resistor in parallel with the amplifier input.

The detection efficiency was measured by the direct counting via NIM scalers of the coincidences between the RPC signal and the trigger signal of the scintillator telescope.

3. Experimental results

For each type of gas we scanned the voltage range from about 0.8 kV below the plateau knee up to 1.2 kV above, and we recorded 100–200 waveforms per voltage.

With the purpose of accounting for the temperature and pressure variations during several weeks data taking, we rescaled the applied voltage V_a according to the relationship $V = V_a \times (P_0/P) \times (T/T_0)$ where T is the laboratory absolute temperature, P the atmospheric pressure and $T_0 = 293\,\mathrm{K}$, $P_0 = 1010\,\mathrm{mbar}$ are arbitrarily defined temperature and pressure reference values [9]. The above formula is based on the hypothesis that gas discharge related phenomena are invariant for any change of V,T,P which leaves the ratio of the voltage to the gas density unchanged.

The relevance of the rescaling is shown in Fig. 2 where the efficiency vs. voltage is given for the binary gas $C_2H_2F_4/C_4H_{10} = 97/3$ at two different pressures (Fig. 2a). The 200 V shift observed between the operating voltages corresponding to the different pressures disappears when the data are plotted vs. the rescaled voltage (Fig. 2b). In the following of this paper all the quoted voltages are normalized with respect to temperature and pressure according to the above formula.

The typical avalanche waveform, shown in Fig. 3a, has an essentially defined time profile with a FWHM of 4 ns. On the contrary the signal amplitude and charge are distributed over a large range.

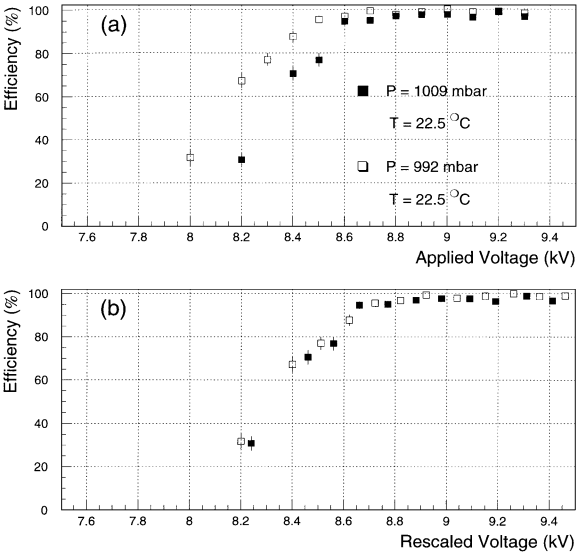

Fig. 2. (a) Detection efficiency vs. the applied voltage for the binary gas mixture, at two different values of the atmospheric pressure. (b) Detection efficiency vs. rescaled voltage for the experimental points shown in (a): the voltage was rescaled using reference values for the atmospheric pressure and temperature, 1010 mbar and 20°C, respectively.

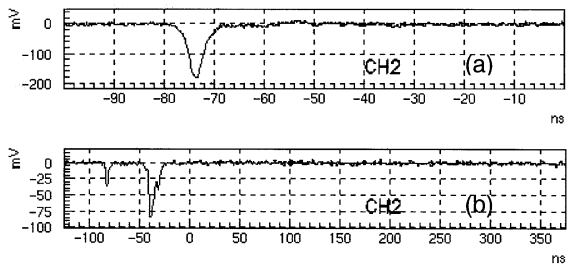

Fig. 3. Waveform samples: (a) avalanche signal at 9.50 kV observed with an amplifier gain of 25; (b) avalanche followed by afterpulses at 10.65 kV (no amplification). The SF_6 concentration is 1%.

Some streamer afterpulses (Fig. 3b, $V = 10.6\,\mathrm{kV}$) are observed at more than 1 kV above the plateau knee. The observed streamer signals have shorter duration with respect to the gas of Ref. [1], and the streamer/avalanche charge ratio is about a factor 6.

The event analysis was carried out according to the following procedure. For each event a "sum waveform" was created by summing the voltages of

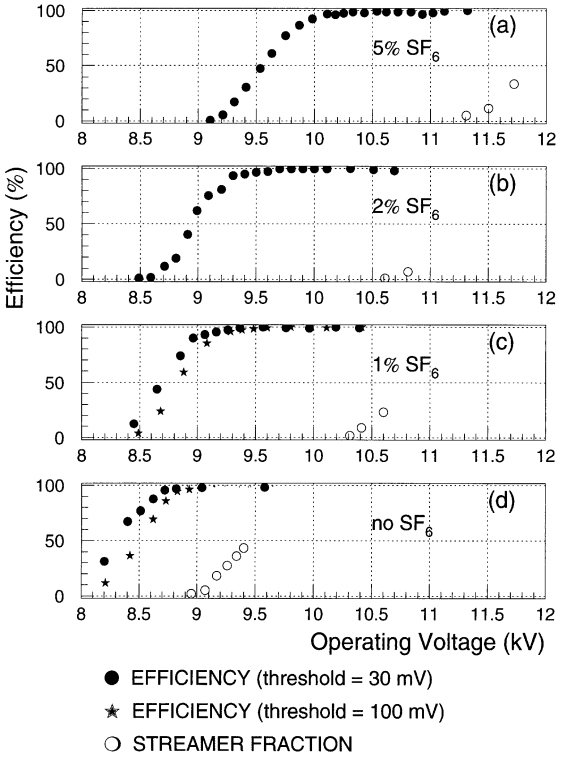

Fig. 4. Detection efficiency and streamer probability vs. operating voltage for (a) 5%, (b) 2%, (c) 1% SF_6 concentrations and (d) no SF_6.

Table 1
50%, 95%, 98% efficiency voltage and streamer threshold for 0%, 1%, 2% and 5% SF_6

SF_6 concentration	$V(50\%)$	$V(95\%)$	$V(98\%)$	V_{stream}
0%	8300	8700	8800	9000
1%	8700	9200	9400	10 300
2%	8950	9400	9600	10 600
5%	9600	10 000	10 300	11 200

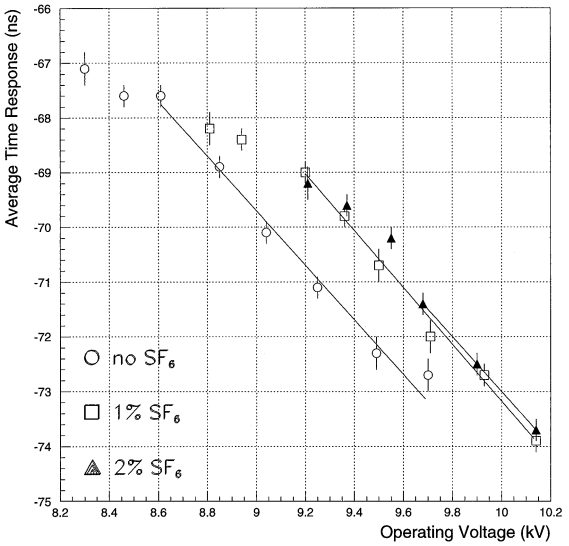

Fig. 5. Average avalanche time delay vs. operating voltage for 2%, 1% SF_6 concentrations and no SF_6.

simultaneous sample points over the three pick-up strips. The sum waveform recombines the currents induced on different strips and it is particularly important for the events in which a cosmic ray crosses the RPC between two contiguous strips. For each sum waveform we recorded the peak times of the avalanche and the streamer pulses (if any), and the limits of the respective time intervals where the signal exceeds the noise. The signal charge was measured as $q = (\Delta t/Z)\sum_i V_i$ where Δt is the sampling time, V_i are the sample voltages inside the selected time interval, and $Z = 25\,\Omega$ is the strip line impedance.

The detection efficiency vs. the operating voltage for 30 mV discrimination threshold (corresponding to about 0.1 mV physical threshold) is shown in Fig. 4a–d for the gas mixtures with 5%, 2%, 1% SF_6 and no SF_6 respectively. The case of 100 mV threshold is reported for 1% SF_6 and no SF_6. The streamer probability measured through the waveform analysis is also reported in the same figure.

The relevant information is summarized in Table 1 which gives, for the three SF_6 concentrations, the voltages of 50%, 95%, and 98% efficiency together with the streamer threshold defined as the voltage giving 1% of streamers. All the three gases containing SF_6 show a ~ 1 kV operating voltage plateau in pure avalanche mode with detection efficiency $> 98\%$.

The avalanche time delay with respect to the trigger signal is shown in Fig. 5 vs. the operating voltage. The rate of change of the time with respect to the voltage is -5.1 ± 0.3 ns/kV for all three SF_6 concentrations.

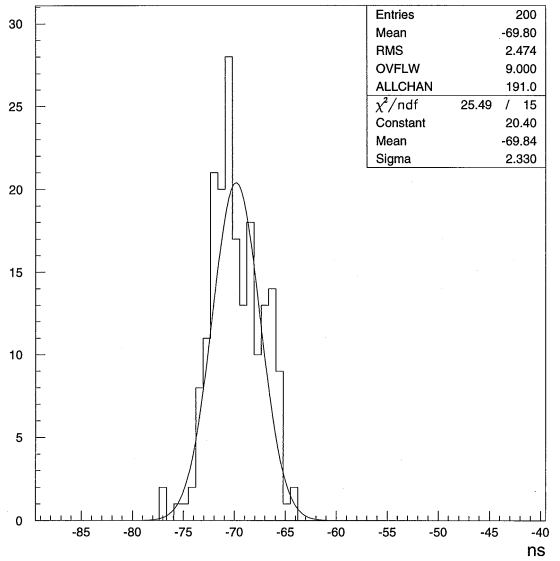

Fig. 6. Distribution of the avalanche peak time (HV = 9.3 kV, 1% SF_6 concentration).

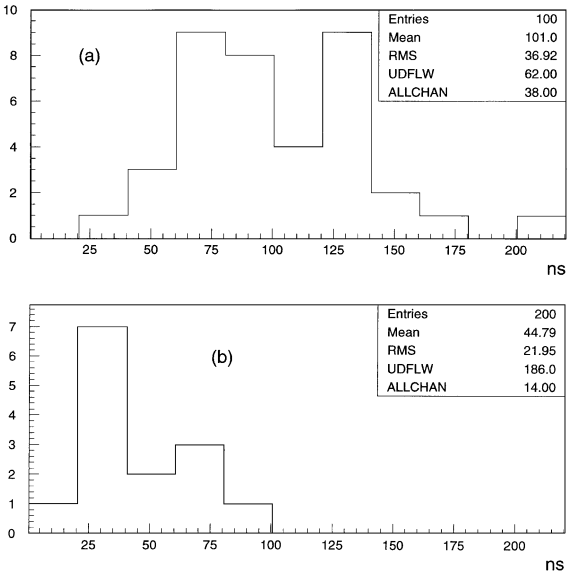

Fig. 7. Avalanche-to-streamer delay distribution for: (a) $C_2H_2F_4/C_4H_{10} = 97/3$ at 9.25 kV; (b) 2% SF_6 at 10.8 kV.

The jitter of the avalanche peak time is shown in Fig. 6. The standard deviation of 2.4 ns is not corrected for the jitter of the trigger signal and the propagation time of RPC signals along the strips.

The distributions of the avalanche-to-streamer delay at voltages moderately above the streamer threshold are shown in Fig. 7 for the gases with no SF_6 (Fig. 7a) and 2% SF_6 (Fig. 7b). The comparison shows that the gas mixtures containing SF_6 produce faster streamers, the average delays being 101 and 45 ns respectively.

The signal charge distributions were studied for all SF_6 concentrations and operating voltages. As an example we show in Fig. 8 the distributions for 2% SF_6 in the range 9.21–10.14 kV. A drastic change in the shape of the distributions for increasing voltage is clearly visible: at low voltage, e.g. 9.21 kV, most of the events are accumulated in the lowest channels and no peak is visible whereas, at 9.68 kV and above, the distributions look peak shaped. This fact, in addition of being very important for practical reasons connected e.g. to the optimization of the frontend electronics, gives a relevant information about the phenomena related to the growth of the discharge in the RPC gas and will be discussed in the next section.

The average value $\langle q \rangle$ of the charge distributions vs. the operating voltage is shown in Fig. 9. For each gas there is an interval where $\ln\langle q \rangle$ increases linearly with the voltage, followed by a region of gradual saturation. The full detection efficiency is reached at the same charge, about 0.6 pC, for all the gases, including the one without SF_6. On the contrary, at the streamer threshold, the charge is 3 pC for all three gases containing SF_6 and only 1 pC for the binary mixture without SF_6. Above the streamer threshold the total signal charge, which is dominated by the streamer, is also plotted in Fig. 9 in addition to the avalanche precursor charge.

For completeness we also show in Fig. 10 the detection efficiency and the streamer probability for the binary gas mixtures $C_2HF_5/C_4H_{10} = 98/2$ and 94/6. The waveform of Fig. 11 shows a streamer pulse following an avalanche precursor with a delay of only 21 ns, suggesting that gas mixtures based on C_2HF_5 are characterized by prompt streamers [3]. This is confirmed by the avalanche-to-streamer delay distribution shown in Fig. 12.

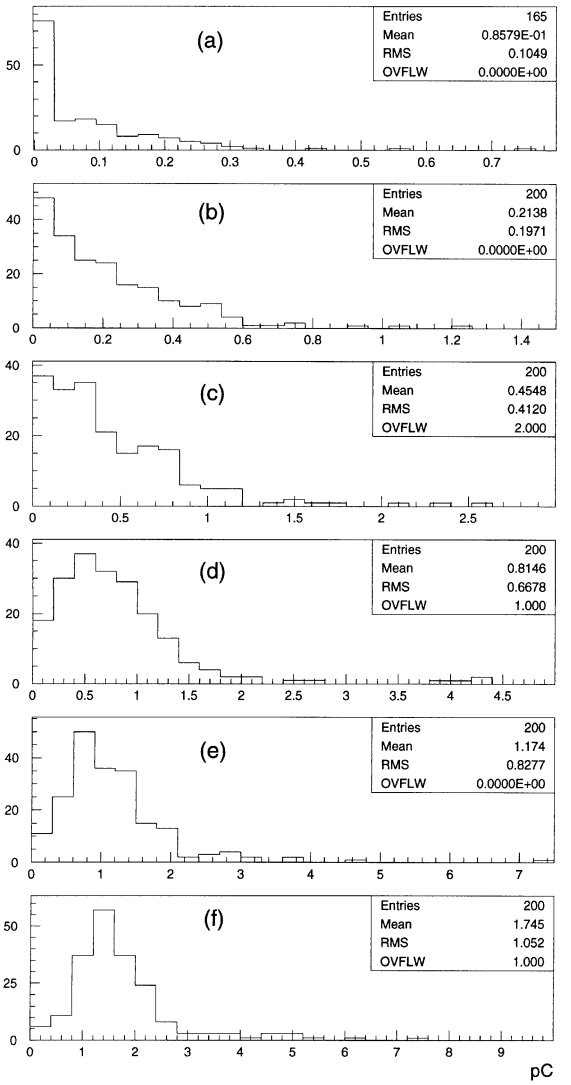

Fig. 8. Avalanche charge distributions for 2% SF_6 and (a) 9.21 kV, (b) 9.37 kV, (c) 9.55 kV, (d) 9.68 kV, (e) 9.90 kV and (f) 10.14 kV.

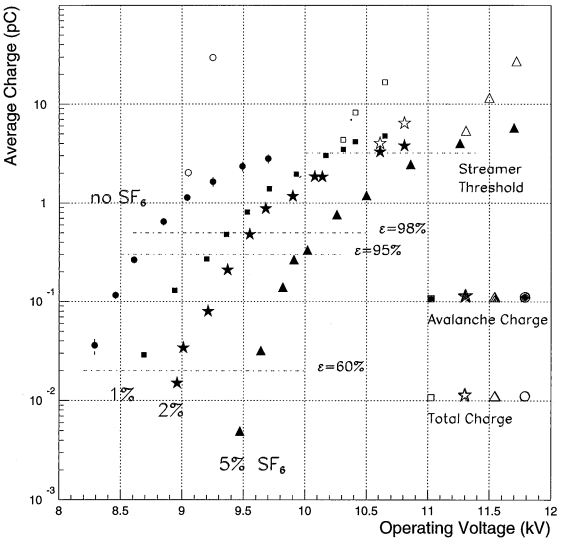

Fig. 9. Average avalanche and total signal charge vs. the operating voltage for the four gases tested.

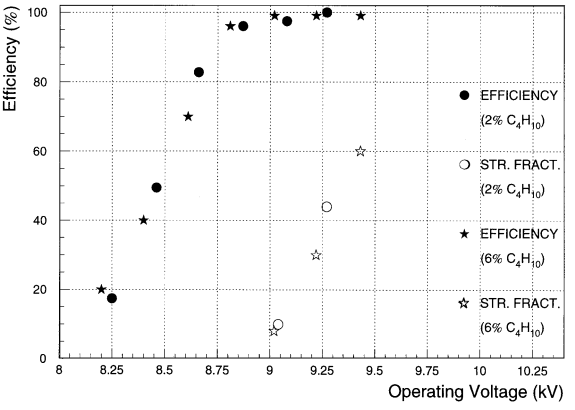

Fig. 10. Detection efficiency (discriminating threshold = 30 mV) and streamer probability for the binary gas mixtures $C_2HF_5/C_4H_{10} = 98/2$ and 94/6.

4. A possible interpretation of the experimental results

A realistic model for describing the electric discharge inside an RPC, and in particular in the conditions of the present test, must explain among other things the behaviour of the charge distribution and its change with the voltage.

In the Townsend discharge, any primary cluster produces an avalanche with a gas gain $e^{\alpha x_i}$ which is strongly dependent on the distance x_i from the anode plane, α being the first Townsend coefficient. The gain increases with the voltage V, due to the fact that α is an increasing function of V. The gain ratio between two clusters, $e^{\alpha(x_i - x_j)}$ also increases with the voltage, so that, in a purely exponential model of the discharge growth, the overall gas gain, for increasing voltage would be asymptotically dominated by the cluster produced closest to the

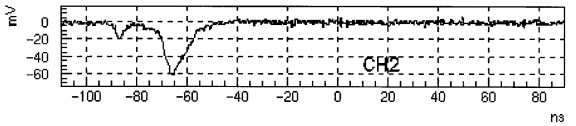

Fig. 11. A typical waveform for the mixture $C_2HF_5/C_4H_{10} = 98/2$ at 9.1 kV; the avalanche signal and the streamer afterpulse are clearly visible.

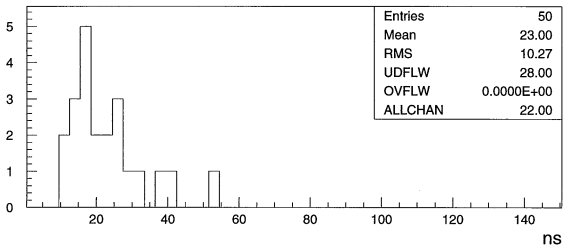

Fig. 12. Avalanche-to-streamer delay distribution at 9.3 kV ($C_2HF_5/C_4H_{10} = 98/2$).

cathode plane. This "largest gain cluster" could give a peak in the charge distribution only if it were produced at an essentially fixed position in the gap, i.e. very close to the cathode. This would require a very high ionization density, which is not the case of the present test. Moreover an increase of the operating voltage would only amplify the signal charge but not change the charge distribution shape. This would be peaked or not depending only on the primary ionization density, not on the operating voltage. Therefore we can conclude that a purely exponential model of the discharge growth cannot explain the charge distributions shown in Fig. 8.

Our data can be explained if we introduce in the model a saturation mechanism, due to the effect of the space charge on the field, which limits the growth of the avalanches. In this case the cluster produced at the maximum distance x_1 from the anode would grow, for increasing voltage, only up to the saturation charge q_{sat}. The following cluster, produced at $x_2 < x_1$, would also grow, for sufficiently large voltage, at the size of q_{sat} and so on. The higher the operating voltage, the larger the number of avalanches reaching the saturated stage would be. A change in the shape of the charge distribution should be observed at the voltage corresponding to the first cluster saturation.

A satisfactory test to decide if this idea can fit or not the experimental data would require an accurate simulation of the discharge development in the gas including also the space charge and saturation phenomena. This simulation is beyond the limits of the present work.

The specific mechanism by which the SF_6 molecule is so effective in suppressing the streamer and how it interferes with the saturation, should be related to its electron affinity of (1.05 ± 0.10) eV [10]. However, this parameter alone is not sufficient to explain the mechanism. Our data suggest that the electron attachment, at the low concentration levels we used, is weak in the first stage of the avalanche growth, as it has only the effect of shifting the operating voltage of a few hundred Volts, and very strong when the avalanche starts to saturate, as it suppresses the transition to streamer. This can be explained if the attachment cross-section is a strongly decreasing function of the field as in the case of Nitrogen/SF_6 mixture [11]. When the space charge effects reduce the field acting on the avalanche the attachment becomes very effective and the existing free electrons generate negative ions which have a much smaller drift velocity and therefore do not contribute any more to the fast signal. This can also explain the streamer suppression if we assume that negative ions are less effective than electrons in radiating high-energy photons when they recombine to positive ions.

Acknowledgements

The authors are endebted to V. Chiostri and L. Di Stante (Università di Roma "Tor Vergata") for their excellent technical support.

References

[1] R. Cardarelli, V. Makeev, R. Santonico, Nucl. Instr. and Meth. A 382 (1996) 470.
[2] ATLAS Muon Spectrometer Technical Design Report, CERN/LHCC/97-22.

[3] E. Cerron Zeballos et al., CERN/LAA-MC 97-01.
[4] R. Cardarelli, Gli RPC come rivelatore di trigger muonico a LHC, Invited talk: LXXXII Congr. Nazionale della Società Italiana di Fisica, Verona, 23–28 settembre 1996.
[5] C. Bacci et al., Nucl. Instr. and Meth. A 352 (1995) 552.
[6] M. Abbrescia et al., Nucl. Phys. B 44 (1995) 218 (Proc. Suppl.).
[7] M. G. Alviggi et al., Resistive Plate Chambers in ATLAS, ATLAS internal note MUON-No-131, 1 October 1996.
[8] R. Cardarelli et al., RPC Front-End Electronics for the ATLAS LVL1 Trigger Detector, in: Proc. of the 7th Pisa Meeting on Advanced Detectors, Isola d'Elba, 25–31 May 1997, Nucl. Instr. and Meth. A 409 (1998) 291.
[9] For rescaling with respect to temperature only, see also: M. Abbrescia et al., Nucl. Instr. and Meth. A 359 (1995) 603.
[10] CRC Handbook of Chemistry and Physics-75th ed. (Editor-In-Chief: D.R. Lide), CRC Press LLC.
[11] J. Phys. B: At. Mol. Opt. Phys. 29 (1996) L713.